Hydrothermal Synthesis of Low-Cost TiO_2: Annealing-Driven Mixed Phase for Enhanced DSSC Performance

Rukhsar Bi Neamat Momin[1], Rahilah Shaikh[2], Rohidas B. Kale[3]
[1,2,3] *Department of Physics, The Institute of Science Dr. Homi Bhabha State University, Fort, Mumbai, 400032, Maharashtra, India.*
doi.org/10.64643/IJIRTV12I3-184136-457

***Abstract*—The TiO_2 nanomaterials were synthesized via a hydrothermal method (T1) and subsequently annealed at 400 °C for 2 h (T2). X-ray diffraction confirmed the formation of pure anatase in T1, while T2 exhibited a mixed anatase–brookite phase along with a reduction in crystallite size. Scanning electron microscopy revealed a stone-like morphology, while annealing induced particle agglomeration, which results in larger aggregates. UV–Vis. spectroscopy showed a slight widening of the band gap, which can be attributed to size quantization effects. Electrochemical analysis demonstrated an enhanced cyclic voltammetry response for the annealed sample. Furthermore, current density–voltage measurements confirmed superior photovoltaic performance, with T2 achieving a power conversion efficiency of 3.68%. These findings highlight the structural, optical, and electrochemical improvements induced by annealing, suggesting the potential of such modified TiO_2 nanomaterials for energy-related applications.**

***Index Terms*—Anatase-Brookite mixed phase; Dye-sensitized solar cells (DSSCs); Hydrothermal method; Renewable energy; TiO_2 nanomaterials.**

I. INTRODUCTION

The global energy crisis is a major challenge of the modern era, as the depletion of conventional resources limits energy availability, disrupts economic stability, and harms environmental sustainability. Solar energy has emerged as a promising renewable alternative, which offers a clean, efficient, and sustainable route to power generation [1]. Among the various types, dye-sensitized solar cells (DSSCs) have attracted considerable attention due to their low fabrication cost, environmental compatibility, and relatively high photo-conversion efficiency (PCE). The conventional DSSC architecture has comprised a TiO_2 nanocrystalline film sensitized with an organic dye as the photoanode (PA), an iodide/triiodide redox couple in a nonaqueous electrolyte, and a platinum (Pt) counter electrode (CE). Despite significant progress, further research is essential to enhance efficiency, stability, and scalability for practical applications [2], [3]. The TiO_2 is widely preferred in the DSSCs due to its abundance, low cost, non-toxicity, and excellent chemical stability. Its large surface area enables efficient dye adsorption, while its favorable band alignment and optical properties make it an effective PA material [4], [5].

In this work, we report the hydrothermal synthesis of low-cost TiO_2 nanomaterials and examined the impact of annealing on their structural, optical, and electrochemical properties. The study aims to optimize TiO_2 as an efficient PA material for enhancing the performance of DSSCs.

II. EXPERIMENTAL PROCEDURE

A. Materials

Titanium isopropoxide (TTIP), acetic acid, chloroplatinic acid (H_2PtCl_6), and N719 dye (Ditetrabutylammonium cis-bis(isothiocyanato) bis(2,2'-bipyridyl-4,4'-dicarboxylato) ruthenium (II)) were purchased from S. D. Fine Chem. Ltd.

B. Methods

In a typical synthesis (Fig. 1), 20 mL of TTIP was added to a mixture of double-distilled water and acetic acid under constant stirring for 2 h. The solution was then heated with stirring until it became transparent, transferred to an autoclave, and treated hydrothermally at 180 °C for 8 h. The obtained product was washed, dried, and labeled as T1. This sample was further annealed at 400 °C for 2 h and labeled as T2.

C. Fabrication of PA and CE

The TiO_2 films were prepared on FTO glass by the doctor blade method using a paste of TiO_2 and ethyl

cellulose (1:4) in propanol to achieve the desired thickness. The films were immersed in an ethanolic solution of N719 dye for two days to prepare the PA. The CE was fabricated by drop-casting H_2PtCl_6 solution onto FTO glass, followed by annealing at 450 °C for 45 min.

D. Fabrication of device

The DSSC was assembled by sandwiching dye-sensitized TiO_2 films as the PA, and Pt-coated FTO as the CE. An electrolyte of lithium iodide and iodine in acetonitrile was introduced into the gap between the electrodes to enable charge transport. The J–V characteristics were recorded under AM 1.5G illumination (100 mW/ cm^2) using a solar simulator.

III. RESULTS AND DISCUSSION

A. Structural Analysis

Figure 2 presents the XRD patterns of synthesized TiO_2 nanomaterials. The diffraction peaks at angle 25.17°, 37.67°, 47.89°, 53.94° and 62.37° of T1 correspond to the anatase phase (JCPDS 21-1272) [6], while the peaks at 25.62°, 38.27°and, 62.96° 2θ values matching the (120), (220), and (160) planes confirm the presence of the brookite phase in T2 (JCPDS 29-1360) [7]. The average crystallite size was estimated using the Debye–Scherrer equation (equation 1) and summarized in Table 1, where notation has usual meaning [8]. A reduction in peak intensity after annealing indicates a decrease in crystallite size.

$$D = \frac{0.9\lambda}{\beta\cos\theta} \qquad \ldots\ldots\ldots\ldots (1)$$

B. Optical Analysis

The UV–Vis. analysis was employed to plot Tauc's plots for TiO_2 material (Fig. 3). The band gap was estimated by extrapolating the linear region of the $(\alpha h\upsilon)^2$ against "energy" curve to the x-axis (α=0). Results showed that a reduction in crystallite size led to an increase in band gap, attributed to nanoscale electron confinement [9]. Therefore, T2 sample has higher bandgap than the T1 sample. The calculated band gap values are listed in Table 1.

C. Morphological Analysis

The scanning electron microscope (SEM) images (Fig. 4) clearly highlight the morphological changes between T1 and T2 samples. In Fig. 4(a-b), the T1 particles appear larger and more agglomerated, with crystallite sizes reaching up to 5.45 μm. After annealing, the T2 sample shows much smaller crystallites in the range of ~860–880 nm (Fig. 4(c-d)), although some larger aggregates are still present (up to ~23 μm). The UV–Vis. analysis further supports these findings, where the bandgap values increase for T2 compared to T1. Thus, the combined SEM and optical results confirm that annealing not only modifies the surface morphology but also plays a key role in tuning the crystallite size and bandgap of TiO_2 nanomaterial, making it more suitable for the DSSC applications.

D. DSSC performance

The Cyclic voltammetry (CV) measurements were carried out using a three-electrode system, where Pt served as the CE, TiO_2 films as the PA, and Ag/AgCl as the reference electrode. The reduction peak intensity was found to be higher for the T2 sample, indicating the presence of more active catalytic sites and improved interfacial charge transfer. As shown in Fig. 5(a), T2 exhibited stronger redox peak currents and a larger enclosed area compared to T1, which can be attributed to its smaller particle size and enhanced catalytic activity at the interface [3]. Fig. 5(b) presents the J-V curves of the DSSCs fabricated with T1 and T2 PA, and the corresponding photovoltaic parameters are summarized in Table 1 under constant illumination (Pin = 100 mW/cm²). The device based on T2 showed higher solar conversion efficiency (η) and fill factor (FF) (equation (2 and 3)) [10], which can be ascribed to reduced crystallite size, larger surface area, and the presence of mixed TiO_2 phases, all of which contribute to improved charge transport and overall DSSC performance.

$$FF = \frac{Jmax\ x\ Vmax}{Jsc\ x\ Voc} \qquad \ldots (2)$$

$$\eta(\%) = \frac{Jsc\ x\ Voc\ x\ FF}{Pin}\ x\ 100 \qquad \ldots (3)$$

IV. CONCLUSION

In this work, nanocrystalline TiO_2 was successfully synthesized by the hydrothermal method, and the influence of annealing on its structural, optical, and photovoltaic properties was systematically investigated for the DSSC applications. The prepared sample (T1) showed anatase phase with larger crystallite size, while the annealed sample (T2) exhibited a reduced crystallite size, higher surface area, and the coexistence of anatase and brookite phases. These modifications improved light absorption, electron transfer, and catalytic activity at

the electrode–electrolyte interface. Electrochemical analysis confirmed that T2 had stronger redox peaks and better charge transport characteristics. When applied as the PA, T2-based DSSC demonstrated higher efficiency (3.68%) compared to T1 (3.06%), owing to enhanced surface reactivity and mixed-phase contribution. Overall, the study highlights the potential of annealed TiO_2 as a cost-effective and efficient PA material for the DSSCs.

V. ACKNOWLEDGMENT

The authors gratefully acknowledge the Department of Science and Technology (DST), India, for the support received under the DST-FIST program (SR/FST/PSI-173/2012), which made this research possible. They are also deeply thankful to the Director and the Institute of Science, Fort, Mumbai, for their continuous encouragement and for providing essential facilities.

REFERENCES

[1] F. Rehman et al., "Fourth-generation solar cells: a review," Jun. 26, 2023, Royal Society of Chemistry. doi: 10.1039/d3ya00179b.

[2] S. Ding, C. Yang, J. Yuan, H. Li, X. Yuan, and M. Li, "An overview of the preparation and application of counter electrodes for DSSCs," Apr. 19, 2023, Royal Society of Chemistry. doi: 10.1039/d3ra00926b.

[3] R. S. Shaikh, R. B. Rajput, S. P, and R. B. Kale, "Significant effects of mesoporus Bi_2S_3/ poly (vinylpyrrolidone) composites on DSSC performance," Current Applied Physics, vol. 55, pp. 22–33, Nov. 2023, doi: 10.1016/j.cap.2023.08.009.

[4] R. B. N. Momin, R. B. Rajput, R. S. Shaikh, and R. B. Kale, "A review of WO_3-based dye-sensitized solar cells: Unveiling the potential of tungsten oxide as counter and working electrodes," Oct. 01, 2024, Elsevier Ltd. doi: 10.1016/j.mssp.2024.108662.

[5] N. Mohite et al., "Facile synthesis of hollow urchin-like Nb_2O_5 nanostructures and their performance in dye-sensitized solar cells," Journal of Solid-State Electrochemistry, vol. 24, no. 2, pp. 273–281, Feb. 2020, doi: 10.1007/s10008-019-04481-5.

[6] A. Deng, Y. Zhu, X. Guo, L. Zhou, and Q. Jiang, "Synthesis of Various TiO_2 Micro-/Nano-Structures and Their Photocatalytic Performance," Materials, vol. 11, no. 6, p. 995, Jun. 2018, doi: 10.3390/ma11060995.

[7] M. Hezam, S. M. H. Qaid, I. M. Bedja, F. Alharbi, M. K. Nazeeruddin, and A. Aldwayyan, "Synthesis of Pure Brookite Nanorods in a Nonaqueous Growth Environment," Crystals (Basel), vol. 9, no. 11, p. 562, Oct. 2019, doi: 10.3390/cryst9110562.

[8] R. B. Rajput and R. B. Kale, "Photocatalytic activity of solvothermally synthesized rutile TiO_2 nanorods for the removal of water contaminants," Materials Science and Engineering: B, vol. 294, p. 116556, Aug. 2023, doi: 10.1016/j.mseb.2023.116556.

[9] S. Bandi, D. Vidyasagar, S. Adil, M. K. Singh, J. Basu, and A. K. Srivastav, "Crystallite size induced bandgap tuning in WO_3 derived from nanocrystalline tungsten," Scr Mater, vol. 176, pp. 47–52, Feb. 2020, doi: 10.1016/j.scriptamat.2019.09.032.

[10] R. S. Shaikh, R. B. Rajput, and R. B. Kale, "Inexpensive green synthesis of natural dye-sensitized solar cells with aqueous solution as a Bi_2S_3 counter electrode," Next Materials, vol. 3, p. 100051, Apr. 2024, doi: 10.1016/j.nxmate.2023.100051.

TABLE AND FIGURES

A. Figures

Fig. 1. Synthesis of TiO_2 by hydrothermal rout.

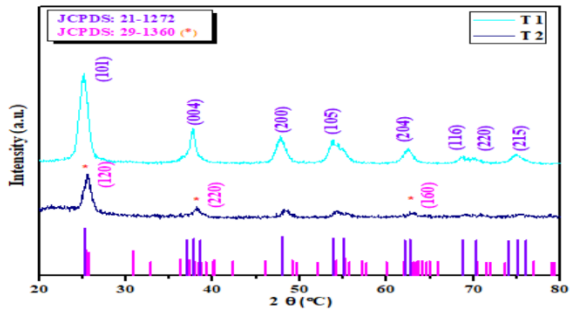

Fig. 2. XRD pattern of TiO_2 nanomaterials

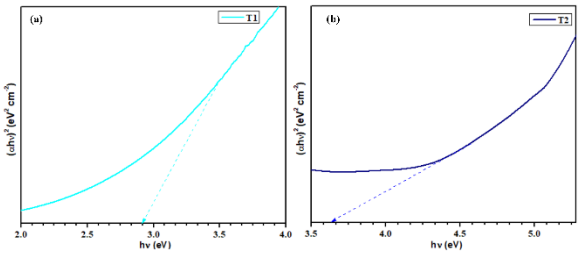

Fig. 3. Tauc Plot of (a) T1 and (b) T2 materials.

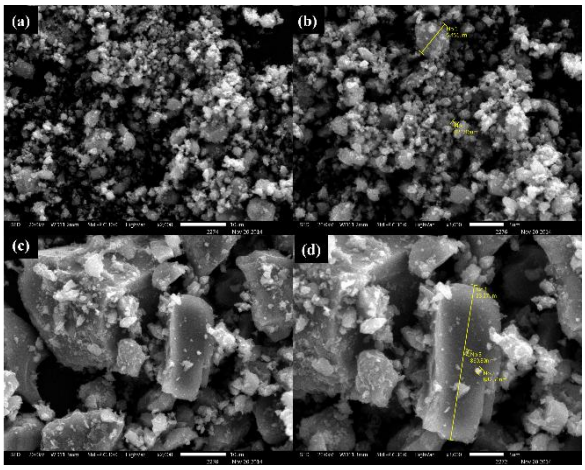

Fig. 4.SEM images of (a-b) T1, and (c-d) T2, at different magnifications.

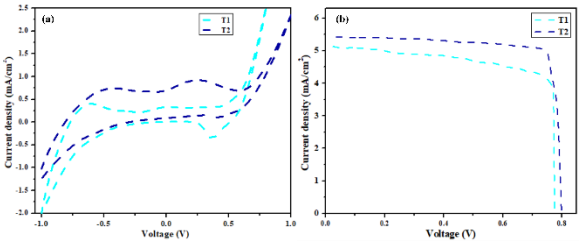

Fig. 5. (a) CV curve (scan rate of 100 mV/s,1 M KOH), and (b) J-V curve, of TiO_2 nanomaterials.

B. Tables

Table 1: The different parameters of T1 and T2 materials.

Sample ID	Crystallite Size (nm)	Band gap (eV)	Voc (V)	Jsc (mA/cm^2)	η (%)	FF
T1	6.47	2.96	0.77	5.12	3.06	0.78
T2	5.68	3.61	0.80	5.38	3.68	0.85